SUPPLEMENTAL MATERIALS.

1) Supplemental Methods

2) Supplemental Tables

3) Supplemental Figures and Figure Legends

4) Supplemental References

Supplemental Methods

TAC DOCA surgery and *Lepr$^{db/db}$* mice

Minimally invasive transverse aortic constriction (TAC) was performed on ~ 12 week old male C57BL/6J mice as described previously with modification[1]. Briefly, mice were anesthetized using a single injection of ketamine and xylazine (120mg/kg and 12mg/kg, I.P.) and a 5mm horizontal incision was made at the first left intercostal space. The thymus was temporarily retracted to visualize the aortic arch and a 7-0 silk suture was passed under the aorta between the right innominate and left carotid arteries. The suture was ligated around a blunted 27 gauge needle and the needle was quickly removed. The chest wall and skin were closed. Sham animals underwent the same procedure except the suture was not ligated around the aorta. An additional incision was made in the right flank of the animal and a subcutaneous pocket was created by blunt dissection. A deoxycorticosterone acetate (50mg/pellet, 21 day release) or placebo pellet (Innovative Research of America) was implanted. The skin was closed and the mice were allowed to recover in a ThermoCare warmer.

Male B6.BKS(D)- *Lepr^{db}/J* mice homozygous for the diabetes spontaneous mutation (*Lepr^{db}*) and heterozygotes (*Lepr^{db}*/+) littermates were purchased from Jackson Laboratories (Bar Harbor, ME). All animal experiments were approved by the Institutional Animal Care and Use Committee (IACUC) at the University of Arizona and the NIH "Using Animals in Intramural Research" guidelines.

In supplemental Table S4 and supplemental Figure S6, the effect of PDE9a inhibition was tested in adult *female* C57BL/6J mice.

Osmotic mini-pumps and vehicle

For chronic inhibition studies. PF-4449613 (Pfizer Inc) was dissolved in 50% dimethyl sulfoxide (DMSO) and 50% polyethylene glycol (PEG) and was administered via subcutaneously implanted osmotic mini-pumps (Alzet osmotic pump, model 2004). Mice were implanted, at 1 week after TAC-DOCA/sham surgery, with osmotic mini-pumps that released PF-4449613 at concentration of 1 or 5 or 8 mg/kg/day for 28 days. The control animals were implanted with osmotic mini-pumps containing vehicle (DMSO and PEG (1:1)) at an equivalent volume. At the end of week 5 after surgery (or the end of week 4 after osmotic mini-pumps implantation), mice were used for invasive hemodynamic assessment.

In *Lepr^{db}* model, male B6.BKS(D)- *Lepr^{db}/J* mice at 3.5 months of age were implanted with osmotic mini-pumps that released PF-4449613 at concentration of 8 mg/kg/day or vehicle for 28 day, then were used for invasive hemodynamic studies.

In supplemental Table S5 and supplemental Figure S7, the effect of early initiation of PDE9a inhibition was tested in adult male C57BL/6J mice. Mice were implanted, at 1 week prior to TAC-DOCA/sham surgery, with osmotic mini-pumps that released PF-4449613 at concentration of 8 mg/kg/day or vehicle and were followed up for 6 weeks. At 5 weeks post-surgery (or the end of week 6 after mini-pumps implantation), mice were used for invasive hemodynamic assessment.

Mouse Echocardiography.

Mice were anesthetized under 2% isoflurane (USP, Phoenix) in oxygen mixture, then placed in dorsal recumbence on a heated platform for echocardiography. Transthoracic echo images were obtained with a Vevo 2100 High Resolution Imaging System (Visual-Sonics, Toronto, Canada) using the model MS550D scan head designed for murine cardiac imaging, and MS250 scan head was used to measure aortic flow velocity at the site of constricted aorta. Care was taken to avoid animal contact and excessive pressure which could induce bradycardia. Body temperature was maintained at 37°C. Imaging was performed at a depth setting of 1 cm. Images were collected and stored as a digital cine loop for off-line calculations. Standard imaging planes, M-mode, Doppler, and functional calculations were obtained according to American Society of Echocardiography guidelines. The parasternal long axis view and mid wall cross sectional view of the left ventricle (LV) were used to guide calculations of percentage fractional shortening, percentage ejection fraction, and ventricular dimensions and volumes. In addition, the left atrial dimension was measured in the long-axis view directly below the aortic valve leaflets. Passive LV filling peak velocity, E (cm/sec), and atrial contraction flow peak velocity, A (cm/sec), were acquired from the images of mitral valve Doppler flow from tilted parasternal long axis views. A

sweep speed of 100 mm/sec was used for M-mode and Doppler studies. Considering that heart rate positively correlates with systolic performance, the heart rates of animals during echocardiographic study were maintained in the range of 500 -550 beats/minute for M-mode, 450-500 beats/minute for B-mode and 400 to 450 beats/minute for Doppler studies.

In-vivo pressure-volume measurements.

An in-vivo pressure-volume analysis was performed in mice using a SciSense Advantage Admittance Derived Volume Measurement System and 1.2F catheters with 4.5 mm electrode spacing (SciSense, London, Ontario, Canada). Mice were anesthetized and ventilated with 2% isoflurane using an SAR-1000 Ventilator (CWE Inc) and body temperature maintained at 37^{o}C using a Mouse Monitor S platform (Indus Instruments). Anesthetized mice were secured and a bilateral subcostal incision was made. The diaphragm was opened to expose the heart. The catheter was inserted into the LV via apical approach. The IVC (inferior vena cava) was located and occluded during a sigh (pause) in ventilation to acquire load-independent indexes. Data acquisition and analysis was performed in LabScribe3 (iWorx, Dover NH). EDPVR was analyzed using a mono-exponential fit ($P = C + Ae^{\beta V}$) with the exponent (β) reported as the stiffness[2].

Treadmill exercise tolerance test

Mice were run on an indirect calorimetry treadmill (TSE Systems) at 5 wk after TAC/DOCA procedure. Mice underwent a graded exercise tolerance test until exhaustion as follows (speed, duration, incline grade): 0 m/min, 3 min, 0°; 6 m/min, 2 min, 0°; 9 m/min, 2 min, 5°; 12 m/min, 2

min, 10°; 15 m/min, 2 min, 15°; 18 m/min, 1 min, 15°; 21 m/min, 1 min, 15°; 23 m/min, 1 min, 15°; and +1 m/min, each 1 min thereafter, 15°. Exhaustion was defined as the point at which mice maintained continuous contact with the shock grid for 5 s or 20 visits to the shock grid in a 1-min period. During testing, gas was collected continuously and analyzed every 5 s. PhenoMaster software (TSE Systems) recorded and calculated oxygen consumption (VO2), carbon dioxide consumption (VCO2), the respiratory exchange ratio (RER), distance run, and visits to the shock grid. The VO2max was determined by the peak VO2 reached during this test when RER was >1.0. Maximum running speed was defined as the treadmill speed at which VO2max was achieved. Mice failing to reach an RER >1.0 were excluded.

Skinned cardiomyocyte passive stiffness measurement

Mouse LV tissues were flash-frozen and stored at -80 °C. Cardiomyocytes were mechanically isolated from frozen LV tissue in cold relaxing solution by Bio-Gen PRO200 homogenizer 5,000 rpm for 30 sec. Mouse cells, isolated as explained above, were skinned for 10 min in relaxing solution with protease inhibitors ([in mmol/L] 0.4 leupeptin, 0.1 E64 , and 0.5 PMSF) and 0.3% Triton X- 100 (Ultrapure; Thermo Fisher Scientific). Cells were washed extensively with relaxing solution pCa 9 and stored on ice. Skinned myocytes were used for mechanic studies within 48 h after time of cell isolation. Myocyte suspension was added to a temperature regulated chamber mounted on the stage of an inverted microscope (Diaphot 200; Nikon). Skinned myocytes were glued at one end to a force transducer (Model 406A, Aurora Scientific). The other end was bent with a pulled glass pipette attached to micromanipulator so that the myocyte axis aligned with the microscope optical axis and cross sectional area (CSA) was measured directly. The cross

sectional images of skinned cells were analyzed using ImageJ Fiji software (National Institutes of Health) and were used to convert measured force to stress. Then, the free end of the cell was glued to a servomotor (Model 315C-I, Aurora Scientific) that imposes controlled stretches. Sarcomere length (SL) was measured with a Video sarcomere length software (VSL 900B, Aurora Scientific) attached to a computer. Passive stress was measured in relaxing solution (pCa 9) with protease inhibitors at 15 °C. Cells were stretched from base length at a speed of 1.0 base length/sec with different stretch amplitude based on % cell length followed by a 20 sec hold and then a release back to the original length. Recovery time of at least 7 min in between stretches was utilized to prevent memory- effects in subsequent measurements. Data were collected using a real-time muscle data acquisition and analysis software (600A, Aurora Scientific) at a sample rate of 2 kHz. Measured forces were converted to stress (force/unit undeformed CSA). To correct for ~20% lattice expansion during skinning process[3], CSA of skinned cells were divided by a correction factor of 1.44. The stress during the 1 base length/sec stretch was plotted against the sarcomere lengths with an exponential fit to derive stress- SL relationships. Passive stress was converted to stiffness (slope of stress-SL relationship). To prevent protein degradation, all solutions contained protease inhibitors ([in mmol/L] 0.01 leupeptin, 0.04 E64, and 0.5 PMSF).

Picro Sirius Red for collagen quantification

Histology with Picrosirius red staining (Picro Sirius Red stain kit, abcam ab 150681) measured the collagen volume fraction in LV cross-sections. The collagen volume fraction (CVF) was measured on tissues fixed in glutaraldehyde. These fixed hearts were sliced radially into sections, embedded, sectioned, and stained using Picrosirius Red to quantify collagen content. Stained

sections were then imaged on a Zeiss microscope (Imager.M1) and analyzed for collagen content using custom Axiovision scripts.

Measurement of PF-4449613 in mouse plasma

PF-4449613 is measured on a liquid-chromatography mass spectrometry system following a simple protein precipitation sample processing method. PF-4449613 stock was prepared in DMSO and diluted in acetonitrile to prepare a calibration curve. Standard concentrations were prepared ranging from a plasma concentration of 10,000 to 2 nM. To prepare the calibration curve, 5µL of standard was added to 25 µL mouse plasma and plasma proteins were precipitated with an additional 60 µL acetonitrile. Plasma samples were processed by protein precipitation with 65 µL acetonitrile. Plasma standards and samples were then vortexed and centrifuged for 10 minutes at 15,600 rcf at 4°C and 10 µL of the supernatant was injected onto the HPLC-MS system for analysis.

PF-4449613 was analyzed on a TSQ Quantum Ultra mass spectrometer with Surveyor HPLC system (ThermoFinnegan, San Jose, CA). The instrument was operated in electrospray ionization (ESI) mode in positive polarity. Instrument parameters were optimized by infusing PF4449613 directly into the ionization source. Quantification of PF-4449613 was done by selected reaction monitoring(SRM)of the transition of the parent (369.1 m/z) to the daughter fragment (176.1 m/z). Chromatographic separation was achieved using a Luna C-18(2) 50X2mm, 5u column (Phenomenex, Torrance, CA) and a gradient system of water(A) and acetonitrile(B), both with 0.1% formic acid (v/v). The initial gradient with a flow rate of 0.2 ml/minute was 10%B, increasing

to 40%B from 3.33 to 4.33 minutes, then increasing to 95%B from 4.33 minutes to 6.33 minutes, holding at 95%B until 7.66 minutes and re-equilibrating at 10% B from 7.7 to 12 minutes.

Adult mouse intact cardiomyocyte isolation.

Cells were isolated as described previously[4]. Briefly, mice were heparinized (1,000 U/kg, i.p.) and euthanized under isoflurane. The heart was removed and cannulated via the aorta with a blunted 21-gauge needle for antegrade coronary perfusion. The heart was perfused for 4 min with perfusion buffer ([in mmol/L] 90 NaCl, 34.7 KCl, 0.6 KH2PO4,0.6 Na2HPO4, 1.2 MgSO4, 12 NaHCO3, 10 KHCO3, 10 HEPES, 10 taurine, 5.5 glucose, 5 BDM,20 Creatine, pH 7.4), followed by digestion buffer (perfusion buffer plus 0.05 mg/ml Liberase TM research grade; Roche Applied Science, and 13 μM $CaCl_2$) for 20 min. When the heart was flaccid, digestion was halted and the heart was placed in myocyte stopping buffer (perfusion buffer plus bovine calf serum 0.08 [BCS]/ml and 8 μM $CaCl_2$) with protease inhibitors ([in mmol/L] 0.4 Leupeptin, 0.1 E64, and 0.5 PMSF (Peptides International, Sigma-Aldrich)). The left ventricle was cut into small pieces, and the rest of the heart was discarded. The small pieces of left ventricle were triturated several times with a transfer pipette and then filtered through a 300 μm nylon mesh filter. Then Ca^{2+} was reintroduced to cardiomyocyte suspension to a final concentration of 1 mM.

Cellular work loop force measurement

All intact cell experiments were performed at temperature 37°C in Medium199 (M5017, Sigma-Aldrich) plus 10 μg/mL insulin (I9278, Sigma-Aldrich). Cells were field-stimulated at 2 Hz frequency by MyoPacer stimulator (IonOptix Co, MA). An inverted microscope (IX-70; Olympus)

was used with a chamber that had platinum electrodes to electrically stimulate cells and a perfusion line with heater control and suction out to maintain a flow rate of ~2 ml/min. All images were recorded with X40 objective lens. Data were collected using an IonOptix FSI A/D board and IonWizard 6.3 software (IonOptix Co, MA) with SarcLen and SoftEdge modules to determine SL and cell width. The sampling frequency of the system was sufficient to measure force (1,000 Hz) and SL (250 Hz) simultaneously. The cellular work loop (the cellular equivalent of PV analysis at the LV chamber level) measurement system which mimics cardiac cycle at the whole heart level[5] (IonOptix LLC) was utilized. A strongly contracting rod-shaped cell was selected, and the glass rods coated with MyoTak (IonOptix Co, MA) were carefully lowered onto opposite ends of the cell. The myocyte was glued at one end to a glass rod that attached to the force transducer (OFT200, OptiForce transducer, IonOptix LLC). The other end of the cell was glued to a glass rod that attached to the piezo translator (Mad City Lab). The cell was slightly pressed between the glass slide and the glass rods, and once attached, the cell was lifted off the glass slide. Cross sectional area of intact cell was obtained from the measured cell width assuming that the cross section of the cell was an ellipse [6]. All forces were normalized to stress.

Cell work loop algorithm was applied through the interface box of the IonOptix system which contains a field programable gate array (FPGA) that digitizes the force signal, and the preload and after load value programed through the IonWizard software 6.3, as described in [5]. The output from the FPGA drove the piezo translator to adjust cell length through a feedback control system based on developed force, implementing preload and afterload. The system constructs force-SL loops by modulating cell length, generating 4 phases that mimic isovolumic contraction, systolic ejection, isovolumic relaxation and diastolic filling phases of the LV chamber[5]. Cellular work loops

reveal systolic and diastolic performance, thus measure the global cardiac function at the single cell level.

Data analysis was performed in LabScribe3 (iWorx, Dover, NH). The ED-SSLR (end diastolic stress-sarcomere length relation) and ES-SSLR (the end systolic stress-sarcomere length relation) were fit with linear relation. The ED-SSLR and ES-SSLR are the cellular analogues of EDPVR (end diastolic pressure volume relation) and ESPVR (end systolic pressure volume relation) of the LV, and reflect cellular diastolic stiffness and systolic contractility, respectively.

To examine the effect of acute PDE9a inhibition in isolated intact cardiomyocytes.

Cellular work loops were conducted, then atrial natriuretic peptide (ANP, Sigma 8208) at final concentration of 1 μM together with PF-4449613 at final concentration of 1 or 5 μM were administered through the cell perfusate (addition of ANP ensures a sufficient level of NP-pGC-cGMP to reveal the effect of PDE inhibition, previous study showed that PF-4449613 at 5 μM inhibited 70% of PDE9a activity with no significant effect on PDE5a activity[7]). After 15 mins in ANP and PF-4449613, cellular work loops were conducted again, and the ED-SSLR and ES-SSLR of the work loops before and after treatment were used for comparison. Previous studies showed that ANP at concentration of 1 μM and PF-4449613 at concentration of 5 μM increased cytoplasmic cGMP of intact cardiomyocytes within ~ 30 sec[7], and the maximal effect of cGMP on intact cardiomyocyte contractility could be observed within 10-15 mins after administration[8], thus we used 15 mins wait time for this experiment. Equivalent volume of DMSO was added to

the cell solution for the control groups. Final concentration of DMSO in cell solution was ~0.025% volume.

RNA analysis RT-PCR.

Total RNA was extracted using the RNeasy Fibrous Tissue Mini Kit with DNase treatment (Qiagen) from left ventricular tissue which upon dissection had been immediately immersed into RNAlater (Ambion) and stored at -20^{o}C. RNA was converted to cDNA using SuperScript™ III First-Strand Synthesis System (Invitrogen). PCR quantification was performed on the LightCycler® 480 Instrument using SYBER Green based Real-Time PCR Master Mix (applied biosystems by Thermo Fisher Scientific). An absolute quantification analysis with a standard curve was used to determine the cDNA concentration of unknown samples. The sequences of the murine primers of each gene are listed below:

Primer Name	**Sequence**
mLoxl1_F1	GGGTAGTGTGTACCGACCCA
mLoxl1_R1	GATGGGCTCTCTGCACGTAT
mLoxl2_F1	GAGCTTTTCTTCTGGGCAAC
mLoxl2_R1	AGCTCCATCCTTGTCCTGTG
mMmp2_L	CCAGCAAGTAGATGCTGCCT
mMmp2_R	GGGGTCCATTTTCTTCTTCA
mCol3a1_R	TAGGACTGACCAAGGTGGCT
mCol3a1_L	GGAACCTGGTTTCTTCTCACC

mCol1a2_F1	AAGGAGTTTCATCTGGCCCT
mCol1a2_R1	AGCAGGTCCTTGGAAACCTT
mANF_L	ATTGACAGGATTGGAGCCCAGAGT
mANF_R	TGACACACCACAAGGGCTTAGGAT
mBNP_L	ACAAGATAGACCGGATCGGA
mBNP_R	ACCCAGGCAGAGTCAGAAAC
MHC7-f	TCCCAAGGAGAGACGACTGTG
MHC7-r	CCTTAAGCAGGTCGGCTGAGT
mTgfβ1_p1	CTCCCGTGGCTTCTAGTGC
mTgfβ1_p2	GCCTTAGTTTGGACAGGATCTG
mSparc_p1	GTGGAAATGGGAGAATTTGAGGA
mSparc_p2	CTCACACACCTTGCCATGTTT
mPolr2a_F3	CTCCCTCTGTTGTTTCTGGG
mPolr2a_R3	TCAAGAGAGTGCAGTTCGGA

Quantitative RT-PCR of *Pde9a* was performed with Light cycler 480 instrument (Roche Life Science) with TaqPath™ 1-Step Multiplex Master Mix (Life technology), TaqMan™Gene Expression Assay (FAM) Assay ID: *Mm00501049_m1 Pde9a and Mm00839502_m1Polr2a*, and the $\Delta\Delta C_T$ analysis method. Specificity of qPCR products was confirmed by melting point analysis. All PCR samples were run in triplicate with *Polr2a* as the reference gene.

Measurement of PDE9a activity in mouse LV myocardium.

PDE9a activity in mouse LV myocardium was assessed as described[9-11] with modifications. Frozen mouse LVs were thawed, washed and homogenized in 0.1 M Tris-HCl buffer containing 2mM $MgCl_2$ and 50 mM NaCl (pH 7.6). Cellular debris was removed by centrifugation of the homogenates at 4°C, at 15,000 g for 15 min. Supernatant was collected for PDE9a activity measurement and protein concentration in supernatant was determined by Bradford protein assay (Bio-Rad). To measure selective PDE9a activity, IBMX (3-Isobutyl-1-methylxanthine) (Sigma I5879) and dipyridamole (Sigma D9766) which are the PDE9a insensitive PDE inhibitors [9, 12, 13] were added to the reaction. The reaction mixture contained, in final concentration, Tris-HCl buffer (0.1 M), $MgCl_2$ (2mM) NaCl (50 mM), dipyridamole and IBMX (100 µM), cGMP (Sigma G6129) and cAMP (Sigma A9501) (50 µM). The mixtures were incubated at 37 °C for 5 mins, 15 mins and 45 mins. The reaction was terminated by the addition of 1.3 M perchloric acid. Then Potassium Phosphate Tribasic was added to the reaction mixture to bring the pH to the range of 5.5-6.5. The reaction mixtures were centrifuged at 30,000 g at 4 °C for 10 mins to get rid of the precipitated protein. The supernatant was collected and one freeze-thaw cycle was applied to induce more protein precipitation. The mixtures were centrifuged again at 30,000 g at 4 °C for 10 mins and the supernatant was collected for HPLC analysis. The level of substrates (cGMP and cAMP) and products (GMP and AMP) were determined by HPLC (Agilent technologies 1200 series) at UV absorbance of 216 and 254 nm. The chromatographic profile of each sample was compared with standard samples and each chromatogram peak was identified by its retention time and DAD spectra. PDE9a-mediated cGMP hydrolysis was determined by the rate of cGMP hydrolysis and GMP generation over time per milligram protein. The cAMP-targeted PDE activity

was determined by the rate of cAMP hydrolysis and AMP generation per milligram protein over time.

Testing PDE9a inhibitory effect of PF-4449613

PDE9a inhibitory effect of PF-4449613 was tested using PDE9a assay kit (BPS Bioscience) as described in the manufactural protocol. The fluorescently labeled cyclic monophosphate (FAM-Cyclic-3',5'-GMP) was incubated with PDE9a protein and PF-4449613 at different concentration, ranging from 0 to 100 µM, for 1 hr. Then the binding agent was added to the reaction mixture. The binding agent selectively bound the phosphate group in the nucleotide product, increasing the size of the nucleotide relative to unreacted cyclic monophosphate. The slowly-rotating nucleotide-bead complexes highly polarized light producing a change in fluorescent polarization that was measured by Biotek 5 instrument, Gen5 (Biotek) microplate reader. Experiment were performed in sextuplicate at each concentration. The result revealed that PF-4449613 is an effective inhibitor of PDE9a with an IC50 of 0.42 µM at substrate (cGMP) concentration of 200 nM and purified PED9a protein 8 pg/µL (Suppl Figure S1).

Quantitative determination of cGMP concentration in mouse plasma.

Mouse blood samples were drawn from right ventricular chambers during terminal procedure under anesthesia, and were stored in EDTA blood tubes. The EDTA whole blood was centrifuged at 5,000 rpm for 10 min, and the plasma was collected. The concentration of cGMP in mouse plasma was determined by parameter cGMP assay kit kge003 (R&D Systems, Minneapolis, MN).

This assay is based on the competitive binding technique in which cGMP present in a sample competes with a fixed amount of horseradish peroxidase (HRP)-labeled cGMP for sites on a rabbit polyclonal antibody. Mouse EDTA plasma samples were diluted 4 times in Calibrator diluent RD5-5 and were assayed according to manufacturer's instructions.

Quantitative determination of PKG activity in mouse LV myocardium.

Mouse LV myocardial samples were homogenized in tissue extraction buffer [50 mM potassium phosphate buffer pH 7.0 with 1mM EDTA, 1mM EGTA,0.2 mM PMSF, 1ug/ml pepstatin, 0.5 ug/ml leupeptin, 5 mM β-glycerophosphate, 2 mM NaF, 2 mM Na_3VO_4, 10 mM β-mercaptoethanol], then were centrifuged for 20 min at 20,000 g. The supernatants were collected and stored at 4 °C. Protein concentration in supernatant was determined by Bradford protein assay (Bio-Rad). The myocardial PKG activity was determined by CycLex cGK assay kit CY-1161 (CycLex Co.,Ltd, Nagano,Japan) in which the PKG in homogenate is allowed to phosphorylate the bound substrate. Then the amount of phosphorylated substrate is measured by binding it with detector antibody and horseradish peroxidase conjugate. The homogenates were diluted to get protein concentration at 0.05 mg/ml, then were assayed according to manufacturer's instructions.

Statistics.

Statistical analysis was performed in Graphpad Prism (GraphPad Software, Inc). Data are shown as mean±SEM. Statistical significance was set at $P<0.05$. * $p\leq0.05$ ** $p\leq0.01$ ***$p\leq0.001$

****p≤0.0001. Normality of data was tested with the D'Agostino & Pearson and Shapiro-Wilk tests. Homogeneity of variance was tested with Brown-Forsythe and Bartlett's test or F-test. For data that were normally distributed with homogeneity of variance, differences between groups were assessed by: the unpaired *t* test (for 2 groups); the one-way ANOVA (for 3 groups); and the two-way ANOVA (for data with 2 controlled variables). For data that were not normally distributed: the Mann-Whitney U test was used to compare 2 groups, the Kruskal–Wallis was used to compare 3 groups; and logarithmic transformation followed by two-way ANOVA was used to compare data with 2 controlled variables. Two-way ANOVA with repeated measures was used to compare the effect before and after acute PF-9613 administration within individual cell. Spearman's rank correlation was used for correlation analysis. The detailed statistical methods used in each experiment are shown in each figure and table legend and are listed as followed: Figures 1D-I, 2D-I, S2A-E and Table S1: two-way ANOVA without repeated measures with a Dunnett test for multiple comparisons of mean of each group with mean of the control group (sham-vehicle or TAC-DOCA-vehicle) was used. Figures 3A-C: The Spearman's rank correlation analysis was used. Figures 4A, 8A: A mono-exponential curve fit and nonlinear regression analysis with a least squares fitting method to determine the differences of individual curve fits among the three experimental groups was used. A non-significant p-value (p>0.05) indicates that one curve can fit all data, while a significant p-value (p≤0.05) indicates that each different data requires its own curve fit. Figures 4D,4F, 6D-I,7D-I,8D, 8F, S3, S4, S5 and Table S3: Two-way ANOVA without repeated measures with a Tukey test for multiple comparisons was performed. Figures 4E: Mann-Whitney U test was used. Figures 5C, 5D, 8E: unpaired t test was used. Figures 4G-H, 8G-H, S6, S7 and Tables S4, S5: One-way ANOVA without repeated measures with a Tukey

multiple comparisons or Kruskal-Wallis with a Dunn test were used as appropriate. Figures 5E-F and Table S2: Two-way ANOVA with repeated measures followed by a Sidak test for multiple comparisons was used to compare the differences in cellular work loop parameters before and after acute PF-9613 administration.

Supplemental Table S1. TAC-DOCA mouse model

	Sham Vehicle	Sham PF-9613 8mg/kg/day	TAC-DOCA Vehicle	TAC-DOCA PF-9613 1mg/kg/day	TAC-DOCA PF-9613 5mg/kg/day	TAC-DOCA PF-9613 8mg/kg/day
Age (days)	123.2±1.1	121.3±0.8	121.1±0.8	125.8±1.8†	119.4±0.1	120±0.4
Body Weight (gm)	30.83±0.42	31.08±0.4	29.38±0.29*	31.41±0.36†	30.88±0.60	29.77±0.52
Tibial Length, TL (mm)	17.5±0.05	17.48±0.07	17.34±0.03*	17.25±0.08*	17.55±0.05	17.35±0.06
Echocardiography						
Number of mice	n=22	n=11	n=40	n=14	n=12	n=19
Heart Rate (bpm)	566.3±7.2	581.5±10.8‡	533±6.2 **	515.3±10.5 ***	543.2±12.7	537.4±9.7
EF (%)	53.98±1.13	51.2±1.01	49.92±1.0	44.63±3.42**	43.07±3.07***	47.42±1.65*
LV EDV (µL)	75.58±2.59	83.65±2.49	77.86±2.41	80.92±3.71	88.63±4.05*	79.11±2.07
LV stroke volume (µL)	40.29±0.95	42.73±1.31‡	37.41±0.63	37.54±1.28	35.97±1.66*	35.21±1.15**
LV diastolic wall strain	0.29±0.01	0.28±0.02	0.23±0.01**	0.22±0.03*	0.21±0.02**	0.23±0.01*
WT;d (mm)	0.75±0.01	0.74±0.02‡‡‡	0.95±0.02****	0.92±0.04****	1.03±0.02****	0.93±0.03****
WT;s (mm)	1.07±0.02	1.02±0.03‡‡‡	1.23±0.02****	1.18±0.04*	1.31±0.04****	1.22±0.03***
LV MPI	0.46±0.01	0.47±0.02	0.45±0.02	0.44±0.02	0.43±0.02	0.44±0.02
Eccentricity	5.47±0.11	5.74±0.12‡‡‡	4.45±0.10****	4.65±0.21***	4.24±0.16****	4.40±0.12****
MV IVRT (msec)	13.19±0.37	13.7±0.54	14.8±0.40	14.99±0.73	14.3±0.77	14.55±0.65
E decel time (ms)	25.72±0.91	25.56±0.65	22.17±0.75**	22.74±1.25	21.16±0.86*	22.66±0.96
MV e' (mm/sec)	22.55±0.85	23.88±1.73‡	18.44±0.56**	17.2±1.21**	18.09±0.86*	17.91±0.80**
MV E/A	1.35±0.04	1.52±0.10	1.77±0.12	1.42±0.06	2.13±0.34**	1.89±0.14*
MV E/e´	34.81±1.46	35.67±1.89	42.7±1.70*	44.05±3.87*	45.61±3.79*	41.14±1.66

Supplemental Table S1 (continue)

	Sham Vehicle	Sham PF-9613 8mg/kg/day	TAC-DOCA Vehicle	TAC-DOCA PF-9613 1mg/kg/day	TAC-DOCA PF-9613 5mg/kg/day	TAC-DOCA PF-9613 8mg/kg/day
Pressure-Volume Analysis						
Number of mice	n=22	n=10	n=33	n=14	n=11	n=15
Load Dependent Parameters						
ESP (mmHg)	87.91±1.44	86.96±3.02‡‡‡	127.4±2.50****	120.8±5.94****	137.1±2.64****	130.2±4.64****
EDP (mmHg)	3.32±0.48	3.19±0.66	6.23±0.63*	6.28±1.01	8.19±1.31**	8.34±1.22***
dPmax (mmHg/s)	9376±328.6	9170±358.4	8299±195*	7976±285.3**	7886±278.2*	8271±370
dPmin (mmHg/s)	-8109±274.3	-8006±399.4	-8417±228.4	-8032±351.5	-7940±548.7	-8284±460.2
ESV (µl)	31.23±1.90	31.25±2.89	41.32±2.07*	40.45±3.39	60.94±5.03****‡‡‡	52.10±5.40****
EDV (µl)	71.25±2.24	70.64±3.02	73.64±2.07	76.09±4.42	91.42±5.02***‡	83.41±5.27
SV (µl)	40.02±1.08	39.40±0.96	34.66±1.04*	35.64±2.21	30.47±2.01***	31.31±1.88***
CO (mL/min)	21.19±0.71	21.28±0.66‡	17.01±0.67***	17.32±1.03*	15.34±1.02***	15.99±0.78***
Tau Weiss (ms)	5.75±0.15	5.86±0.22†	7.08±0.21***	6.64±0.20	8.12±0.64****	7.67±0.50****
Ea (mmHg/µl)	2.25±0.07	2.24±0.10‡‡‡	4.03±0.19****	3.66±0.35***	4.71±0.35****	4.32±0.31****
VA coupling ratio	0.59±0.05	0.7±0.11	0.82±0.06	0.62±0.07	1.19±0.16****†	1.06±0.12***
Load Independent Parameters						
Ees (mmHg/µl)	4.13±0.31	3.78±0.51	5.46±0.28*	6.38±0.59***	3.98±0.38†	4.49±0.42†
PRSW (mmHg)	92.83±2.01	88.99±3.59‡	112±3.76**	114.3±5.05**	93.56±7.07†	99.98±6.03
EDPVR (mmHg/µl)	0.020±0.002	0.022±0.004‡	0.045±0.004****	0.038±0.005*	0.028±0.003†	0.029±0.004†
Tissue Morphometry						
Number of mice	n=26	n=10	n=46	n=14	n=12	n=15
LV/TL (mg/mm)	5.35±0.08	5.56±0.07‡‡‡	7.94±0.19****	7.51±0.40****	9.18±0.44****‡	8.28±0.42****
RV/TL (mg/mm)	1.32±0.03	1.34±0.04	1.31±0.03	1.35±0.04	1.41±0.09	1.40±0.05
Lt ATR/TL(mg/mm)	0.23±0.01	0.24±0.01‡‡	0.40±0.02****	0.42±0.041****	0.52±0.06****†	0.48±0.05****
Rt ATR/TL(mg/mm)	0.23±0.01	0.22±0.01	0.26±0.01	0.26±0.02	0.28±0.02	0.29±0.02**
Lung/TL(mg/mm)	8.42±0.17	8.97±0.02	11.2±0.79*	10.06±1.05	N/A	10.02±0.82

Supplemental Table S1. Echocardiography, pressure volume analysis parameters and tissue morphometry of TAC-DOCA mice after 4 weeks of vehicle or PDE9a inhibition. ATR indicates atria; CO, cardiac output; d, diastole; dPmax, maximal rate of pressure change; dPmin, minimal rate of pressure change; Ea, effective arterial elastance; EDP, end-diastolic pressure; EDPVR, end-diastolic pressure-volume relation; EDV, end-diastolic volume; Ees, end-systolic elastance; EF, ejection fraction; ESP, end-systolic pressure; ESV, end-systolic volume; IVRT, isovolumic relaxation time; LA, left atrium; LV, left ventricle; LVID, LV internal dimension; MPI, myocardial performance index; MV, mitral valve; PRSW, preload recruitable stroke work; PV, pressure-volume; RV, right ventricle; S, systole; SV, stroke volume; Tau Weiss, left ventricular relaxation–time constant; TL, tibial length; VA coupling ratio (Ea/Ees),ventricular-arterial coupling ratio; and WT, wall thickness.* p≤0.05,** p≤0.01, ***p≤0.001, ****p≤0.0001 significant vs. sham vehicle, ǂ p≤0.05,ǂǂ p≤0.01, ǂǂǂp≤0.001, ǂǂǂǂ p≤0.0001 significant vs. TAC-DOCA-veh. Data were analyzed by two-way ANOVA without repeated measures followed by a Dunnett test.

	Sham		Sham		TAC DOCA		TAC DOCA		TAC DOCA	
	baseline	after vehicle	baseline	after PF-9613 5 µM ANP 1 µM	baseline	after vehicle	baseline	after PF-9613 1 µM ANP 1 µM	baseline	after PF-9613 5 µM ANP 1 µM
Diastolic stress [mN/mm^2]	0±0.17	0.24±0.2	0±0.26	0.44±0.37	0±0.09	0±0.15	0±0.08	0.44±0.28	0±0.15	0.11±0.17
Stress development velocity [mN/mm^2.sec]	58.89±5.67	55.03±7.43	48.4±7.09	36.4±6.23	61.96±11.95	71.37±13.8	50.19±7.90	63.89±12.74	87.83±13.3	89.12±16.64
Stress development velocity/ stress amplitude	50.28±2.69	48.54±2.73	45.98±4.85	40.87±6.77	41.63±3.39	44.89±3.17	28.15±1.59	34.37±2.72	42.85±1.91	42.32±1.54
Stress amplitude [mN/mm^2]	1.19±0.12	1.12±0.12	1.12±0.24	0.93±0.15	1.52±0.24	1.65±0.34	1.8±0.27	2.18±0.63	2.07±0.33	2.08±0.39
Stress decay velocity [mN/mm^2.sec]	-47.08±6.67	-45.4±5.63	-42.08±8.07	-44.17±14.45	-56.93±10.99	-70.47±12	-54.74±14.62	-47.51±8.95	-77.04±11.94	-83.51±17.42
Stress decay velocity/ stress amplitude	-38.55±2.3	-40.17±3.09	-38.38±4.45	-45.73±12.42	-43.34±8.26	-50.93±8.86	-37.78±8.43	-29.97±2.03	-36.77±2.65	-38.56±4.3
Time to 50% peak stress [msec]	18.71±1.78	19.14±1.81	20±1.48	24.2±2.48 **	21.9±2.12	21.2±1.91	29.0±0.01	25.3±0.01	20.69±1.01	21.77±1.04
Time to 50% stress decay [msec]	21.29±1.19	20.43±1.78	21.4±2.66	28.6±8.58	25.44±2.76	22.11±1.59	44.0±0.01	27.0±0.03****	23±1.32	23.77±1.57
ED-SSLR [mN/mm^2.µm]	10.47±2.33	10.89±3.08	9.97±2.7	10.28±2.49	23.81±4.08	26.58±4.88	27.12±3.39	30.72±4.31*	23.43±2.91	24.61±3.03
ED-SSLR X intercept [µm]	1.77±0.01	1.76±0.01	1.77±0.01	1.72±0.03**	1.78±0.02	1.78±0.03	1.72±0.02	1.71±0.02	1.84±0.03	1.85±0.02
ES-SSLR [mN/mm^2.µm]	26.53±3.28	30.01±6.73	23.77±2.78	24.18±3.26	59.33±7.39	62.8±8.14	65.43±9.58	73.76±11.52	55.47±7.36	58.11±7.55
ES-SSLR X intercept [µm]	1.72±0.01	1.72±0.02	1.72±0.02	1.69±0.03	1.71±0.01	1.88±0.18	1.68±0.01	1.66±0.01	1.77±0.02	1.78±0.02
PRSW [mN/mm^2]	1.41±0.34	1.54±0.35	1.64±0.34	1.54±0.33	2.04±0.66	2.04±0.57	1.74±0.28	2.01±0.27	2.35±0.54	2.61±0.64

Supplemental Table S2. Testing the effect of acute PDE9a inhibition in intact cardiomyocytes. ED-SSLR indicates end diastolic stress-sarcomere length relation; ES-SSLR, end systolic stress-sarcomere length relation; PRSW, preload recruitable stroke work. n= 6,7,10,10,13 cells from 3,3,8,5,6 mice. * p≤0.05,** p≤0.01, ***p≤0.001, ****p≤0.0001 significant vs. baseline. Data were analyzed by repeated measures two-way ANOVA followed by a Sidak test.

Supplemental Table S3. *Lepr^{db}* mouse model

	Lepr^{db}/+ Vehicle	*Lepr^{db}*/+ PF-9613 8 mg/kg/day	*Lepr$^{db/db}$* Vehicle	*Lepr$^{db/db}$* PF-9613 8 mg/kg/day
Age (days)	132.3±2.4	132.4±2.4	131±2.3	132.2±3.0
Body Weight, BW (gm)	35.03±0.40	34.74±0.48	57.48±0.81****‡‡‡‡	58.24±1.11****‡‡‡‡
Tibial Length, TL (mm)	17.41±0.10	17.38±0.06	16.65±0.12****‡‡‡‡	16.46±0.10****‡‡‡‡
Echocardiography				
Number of mice	n=17	n=16	n=20	n=17
Heart Rate (bpm)	576.1±6.7	568.9±8.6	509.3±10.2****‡‡‡‡	508.1±11.9****‡‡‡‡
Cardiac output (mL/min)	29.16±1.05	27.7±0.98	23.89±0.70***‡	24.01±0.91**‡
EF (%)	53.34±1.62	52.98±1.54	61.78±1.28***‡‡‡	63.94±1.52****‡‡‡‡
LV EDV (µL)	96.38±4.35	93.19±4.05	77±2.98**‡‡	74.71±2.73***‡‡
LV stroke volume (µL)	49.22±1.41	48.68±1.46	47.06±1.34	47.49±1.66
LV diastolic wall strain	0.26±0.02	0.27±0.02	0.29±0.01	0.31±0.02
WT;d (mm)	0.76±0.02	0.75±0.01	0.72±0.01	0.75±0.02
WT;s (mm)	1.03±0.02	1.03±0.02	1.02±0.02	1.09±0.03
LV MPI	0.46±0.02	0.47±0.02	0.48±0.02	0.47±0.02
Eccentricity	5.96±0.22	5.92±0.11	5.70±0.18	5.54±0.18
MV IVRT (msec)	12.83±0.51	13.67±0.71	15.44±0.45**	15.37±0.54*
E decel time (ms)	28.22±0.54	26.71±0.82	25.27±0.96	24.02±1.09*
MV e' (mm/sec)	27.14±1.12	24.8±1.46	17.93±0.92****‡‡‡‡	17.69±1.01****‡‡‡‡
MV E/A	1.37±0.09	1.41±0.06	1.56±0.13	1.48±0.07
MV E/e´	28.4±1.30	29.57±1.41	36.68±1.92**‡	37.14±1.65**‡

Supplemental Table S3 (continue)

	Lepr^{db}/+ Vehicle	*Lepr*^{db}/+ PF-9613 8 mg/kg/day	*Lepr*$^{db/db}$ Vehicle	*Lepr*$^{db/db}$ PF-9613 8 mg/kg/day
Pressure-Volume Analysis				
Number of mice	n=9	n=9	n=9	n=8
Load Dependent Parameters				
ESP (mmHg)	90.13±2.38	94.51±2.57	114.42±4.34****‡‡	108.41±3.42**†
EDP (mmHg)	2.84±0.77	3.32±0.71	10.37±1.86**‡	7.90±1.68
dPmax (mmHg/s)	8862±293	9123±447	10,001±891	10,032±432
dPmin (mmHg/s)	-7996±407	-8419±423	-8267±751	-7881±407
ESV (µl)	40.31±2.92	31.13±3.22	41.59±3.41	35.12±3.54
EDV (µl)	85.66±4.43	74.59±3.58	85.09±4.79	76.64±4.58
SV (µl)	45.34±3.10	43.46±1.97	43.5±2.21	41.52±2.73
Tau Weiss (ms)	6.25±0.32	5.93±0.33	9.00±1.08*†	8.14±0.61
Ea (mmHg/µl)	2.09±0.15	2.23±0.11	2.72±0.16*	2.73±0.21*
VA coupling ratio	0.70±0.06	0.60±0.04	1.02±0.12†	1.10±0.15*‡
Load Independent Parameters				
Ees (mmHg/µl)	3.11±0.26	3.96±0.46	2.96±0.40	2.66±0.26
PRSW (mmHg)	87.72±3.97	86.18±4.39	86.54±6.36	84.84±4.89
EDPVR (mmHg/µl)	0.019±0.002	0.023±0.004	0.044±0.007**†	0.035±0.005
Tissue Morphometry				
Number of mice	n=9	n=9	n=9	n=9
LV/TL (mg/mm)	6.47±0.20	6.19±0.24	5.81±0.17	5.89±0.12
RV/TL (mg/mm)	1.64±0.10	1.61±0.07	1.44±0.05	1.49±0.06
Lt ATR/TL (mg/mm)	0.29±0.02	0.26±0.01	0.23±0.02	0.23±0.02
Rt ATR/TL (mg/mm)	0.33±0.01	0.28±0.02	0.27±0.03	0.25±0.01*
Lung/TL (mg/mm)	9.30±0.18	9.31±0.23	8.09±0.25**‡	8.43±0.19*†

Supplemental Table S3. Echocardiography, pressure volume analysis parameters and tissue morphometry of *Lepr*$^{db/db}$ mice after 4 weeks of vehicle or PF-9613 treatment For abbreviation, please refer to Table S1.* p≤0.05 ** p≤0.01 ***p≤0.001 ****p≤0.0001 significant vs. *Lepr*^{db}/+veh, ŧ p≤0.05,ŧŧ p≤0.01, ŧŧŧp≤0.001, ŧŧŧŧ p≤0.0001 significant vs. *Lepr*^{db}/+ inh. Data were analyzed by two-way ANOVA without repeated measures followed by a Tukey test.

Supplemental Table S4. A study in *female* TAC-DOCA mouse model

	Sham Vehicle	TAC-DOCA Vehicle	TAC-DOCA PF-9613 8 mg/kg/day
Age (days)	122.8 ± 4.8	134.6 ± 5.7	134.0 ± 5.8
Body Weight,BW (gm)	22.1 ± 1.7	26.0 ± 0.5*	24.8 ± 0.5
Tibial Length, TL(mm)	17.1 ± 0.3	17.2 ± 0.2	17.1 ± 0.3
Pressure-Volume Analysis	n=4	n=7	n=7
Load Dependent Parameters			
ESP (mmHg)	80.7 ± 3.3	114.3 ± 3.4*	127.8 ± 9.4**
EDP (mmHg)	2.5 ± 1.0	4.8 ± 0.8	3.5 ± 0.4
dPmax (mmHg/s)	8897 ± 842	6624 ± 331*	8834 ± 424 ǂ
dPmin (mmHg/s)	-6429 ± 291	-7360 ± 406	-9322 ± 397***ǂ
ESV (µl)	23.5 ± 3.4	35.1 ± 3.7	33.5 ± 3.4
EDV (µl)	57.7 ± 6.8	69.0 ± 5.4	67.7 ± 3.7
SV (µl)	34.2 ± 3.6	33.8 ± 3.0	34.3 ± 3.0
CO (mL/min)	19.37 ± 1.82	16.18 ± 1.60	16.96 ± 1.56
Tau Weiss (ms)	6.4 ± 0.3	7.4 ± 0.3	6.1 ± 0.2 ǂ
Ea (mmHg/µl)	2.50 ± 0.36	3.49 ± 0.24	3.48 ± 0.31
VV coupling ratio	0.41 ± 0.06	0.54 ± 0.05	0.77 ± 0.17
Load Independent Parameters			
Ees (mmHg/µl)	6.26 ± 0.61	6.45 ± 0.78	5.91 ± 0.29
PRSW (mmHg)	84.39 ± 1.91	106.04 ± 8.60	113.70 ± 5.58*
EDPVR(mmHg/µl)	0.025 ± 0.004	0.063 ± 0.016	0.038 ± 0.011
Tissue Morphometry	n=5	n=8	n=7
LV/TL (mg/mm)	4.09 ± 0.26	6.35 ± 0.24***	6.76 ± 0.44***
RV/TL (mg/mm)	1.18 ± 0.08	1.48 ± 0.03**	1.60 ± 0.04****
Lt ATR/TL (mg/mm)	0.15 ± 0.01	0.29 ± 0.02**	0.33 ± 0.03***
Rt ATR/TL (mg/mm)	0.15 ± 0.01	0.20 ± 0.01	0.22 ± 0.02**

Supplemental Table S4. Pressure volume analysis and tissue morphometry in a study of f*emale* TAC-DOCA mice. For abbreviation, please refer to table 1.* p≤0.05 ** p≤0.01 ***p≤0.001 ****p≤0.0001 significant vs sham, ǂ p≤0.05,ǂ p≤0.01, ǂǂp≤0.001, ǂǂǂ p≤0.0001 significant vs TAC-DOCA vehicle. Data were analyzed by one-way ANOVA followed by a Tukey test or Kruskal-Wallis followed by a Dunn test.

Supplemental Table S5. A study of <u>early initiation of PDE9a inhibition</u>

	Sham Vehicle	TAC-DOCA Vehicle	TAC-DOCA PF-9613 8 mg/kg/day
Age (days)	131 ± 3.2	136.3 ± 3.2	138.3 ± 3.0
Body Weight,BW (gm)	30.6 ± 1.9	29.0 ± 0.4	29.8 ± 0.9
Tibial Length, TL(mm)	17.1 ± 0.2	17.1 ± 0.1	16.9 ± 0.1
Pressure-Volume Analysis	n=5	n=8	n=10
Load Dependent Parameters			
ESP (mmHg)	95.13 ± 5.24	116.2 ± 3.78*	120.4 ± 4.60**
EDP (mmHg)	3.05 ± 0.62	4.69 ± 0.83	4.68 ± 0.57
dPmax (mmHg/s)	9044 ± 348	6576 ± 459*	7646 ± 550
dPmin (mmHg/s)	-8515 ± 353	-7309 ± 686	-8250 ± 515
ESV (µl)	28.44 ± 4.07	51.59 ± 5.86*	41.19 ± 5.21
EDV (µl)	69.62 ± 7.56	85.61 ± 6.64	77.47 ± 5.67
SV (µl)	41.17 ± 4.22	34.03 ± 2.45	36.28 ± 1.49
CO (mL/min)	20.26 ± 1.50	15.39 ± 1.25*	16.6 ± 0.99
Tau Weiss (ms)	5.90 ± 0.21	8.02 ± 0.83	6.92 ± 0.43
Ea (mmHg/µl)	2.40 ± 0.18	3.65 ± 0.40*	3.41 ± 0.18
VV coupling ratio	0.81 ± 0.08	0.91 ± 0.07	0.81 ± 0.05
Load Independent Parameters			
Ees (mmHg/µl)	2.81 ± 0.17	4.08 ± 0.38	4.50 ± 0.41
PRSW (mmHg)	79.33 ± 3.51	90.8 ± 5.17	97.6 ± 6.52
EDPVR(mmHg/µl)	0.019± 0.004	0.046 ± 0.004**	0.036 ± 0.004*
Tissue Morphometry	n=5	n=9	n=11
LV/TL (mg/mm)	5.02 ± 0.21	7.52 ± 0.72*	7.39 ± 0.50*
RV/TL (mg/mm)	1.47 ± 0.09	1.54 ± 0.06	1.63 ± 0.08
Lt ATR/TL (mg/mm)	0.21 ± 0.02	0.29 ± 0.05	0.33 ± 0.03
Rt ATR/TL (mg/mm)	0.20 ± 0.03	0.24 ± 0.04	0.21 ± 0.01

Supplemental Table S5. Pressure volume analysis and tissue morphometry in *male* TAC-DOCA mice with <u>early initiation of PDE9a inhibition</u>. For abbreviation, please refer to table 1.* p≤0.05 ** p≤0.01 ***p≤0.001 ****p≤0.0001 significant vs sham vehicle, ǂ p≤0.05,ǂǂ p≤0.01, ǂǂǂp≤0.001,

ǂǂǂ p≤0.0001 significant vs TAC-DOCA vehicle. Data were analyzed by one-way ANOVA followed by a Tukey test or Kruskal-Wallis followed by a Dunn test.

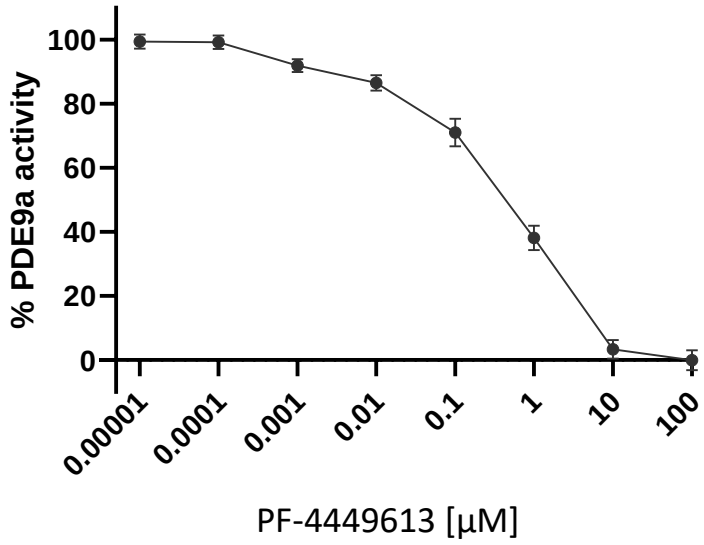

Supplemental Figure S1. Inhibition of PDE9a activity by PF-04449613. Inhibition of PDE9a activity by PF-4449613 is demonstrated. PF-4449613 is an effective inhibitor of PDE9a with an IC50 of 0.42 µM at substrate (cGMP) concentration of 200 nM and purified PED9a protein 8 pg/µL. Data performed in sextuplicate for each concentration.

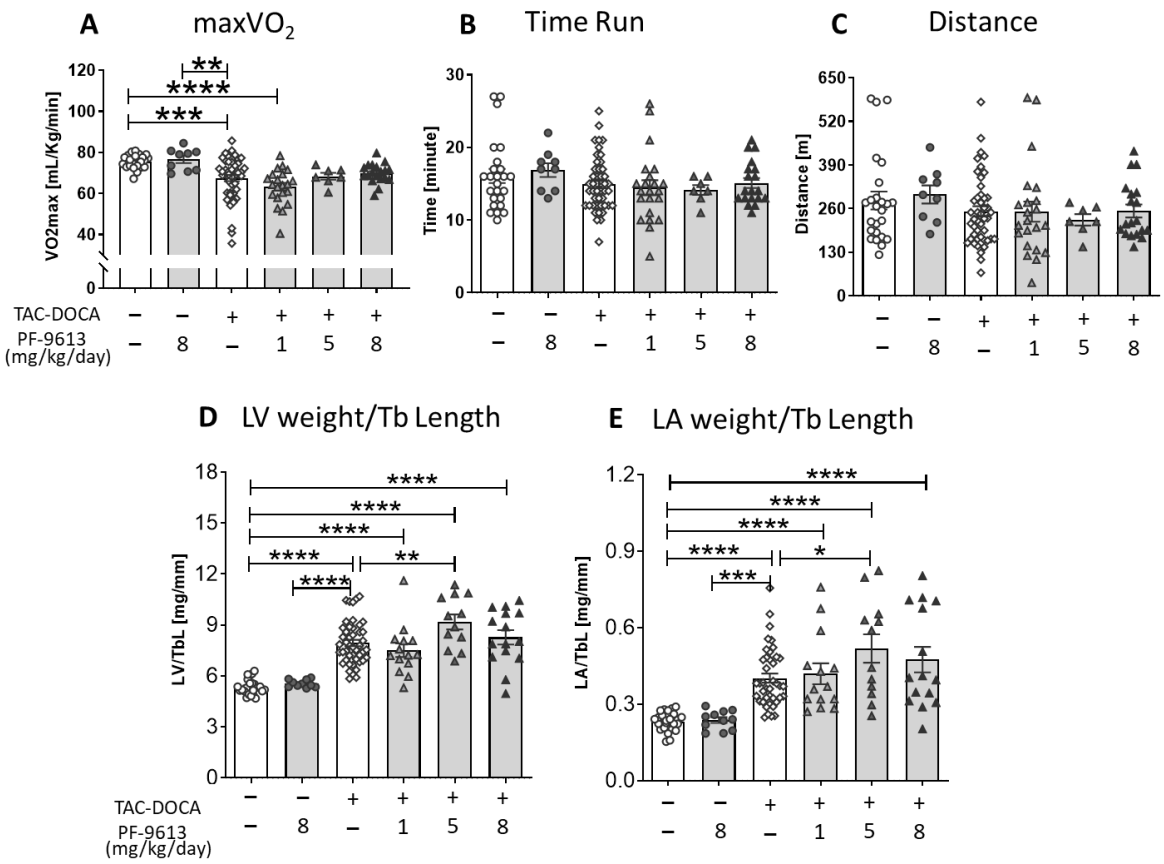

Supplemental Figure S2. Treadmill exercise test (A-C) shows a reduced peak O_2 consumption (maxVO2) in TAC-DOCA-veh and TAC-DOCA-inh1 relative to sham mice. There are no improvement in maxVO2 **(A)** in any groups of TAC-DOCA-inh compared to TAC-DOCA-veh. There are no differences in time run **(B)** or distance **(C)** among groups (n=25,9,46,21,7,19). **Tissue morphometry of TAC-DOCA mice (D&E)** Normalized LV weight **(D)** and LA weight **(E)** are increased in all TAC-DOCA groups compared to sham mice. No attenuations of LV or LA hypertrophic responses are observed after chronic PDE9a inhibition (n = 26, 10, 46, 14, 12, 15). * p≤0.05 ** p≤0.01 ***p≤0.001 ****p≤0.0001. Data were analyzed by two-way ANOVA without repeated measures followed by a Dunnet test.

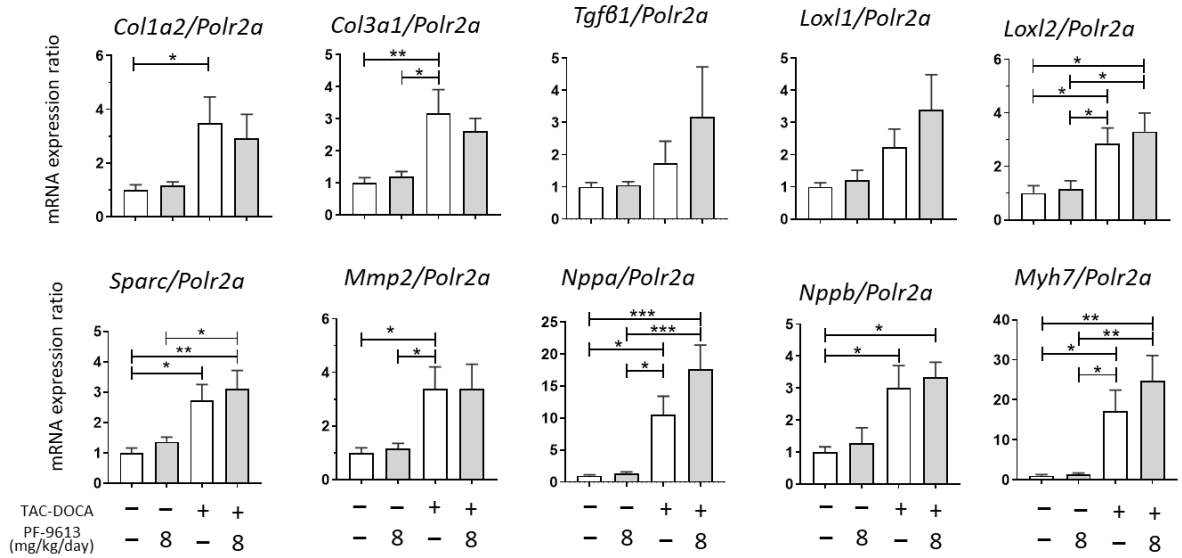

Supplemental Figure S3. RNA expression of fibrosis associated genes and fetal gene markers in TAC-DOCA mouse model with PDE9a inhibition. qRT PCR was used to quantify expression of fibrosis associated genes (*Col1a2, Col3a1, Tgfb1, Mmp2, Loxl1, Loxl2* and *Sparc*) as well as fetal gene markers (*Nppa, Nppb and MyH7*) in LV myocardium of TAC-DOCA mouse models with *Polr2a* as the reference gene. TAC-DOCA mice exhibit significantly elevated mRNA expression of *Col1a2, Col3a1, Loxl2, Sparc, Mmp2,* and increasing trends of *Tgfb1 and Loxl1* expression. There are significant upregulations of fetal gene markers (*Nppa, Nppb* and *Myh7)* in both groups of TAC-DOCA mice. However, there are no differences in expression of fibrosis associated genes or fetal marker genes between TAC-DOCA vehicle and TAC-DOCA with PDE9a inhibition, suggesting no effect of PDE9a inhibition on fibrotic phenotype or fetal genes at the transcript level.* p≤0.05 ** p≤0.01 ***p≤0.001, n = 6,7,6,5 mice. Data were analyzed by two-way ANOVA without repeated measures followed by a Tukey test.

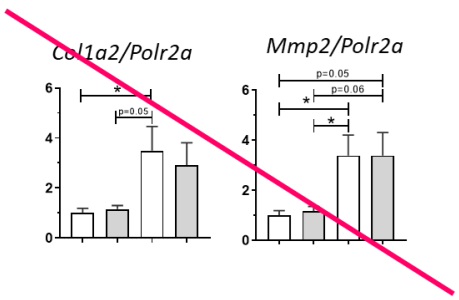

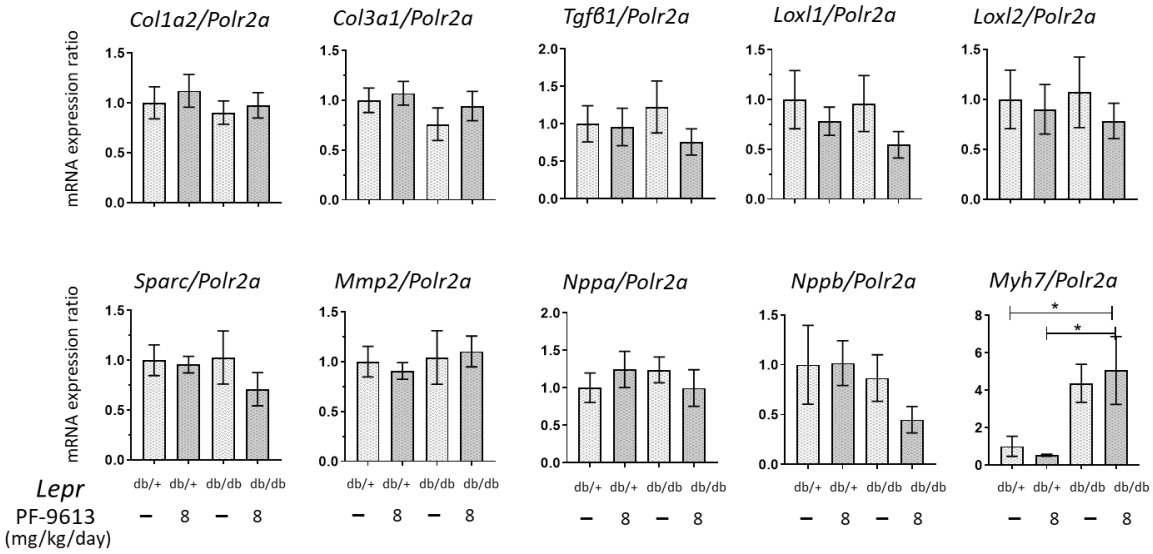

Supplemental Figure S4. RNA expression of fibrosis associated genes and fetal gene markers in *Lepr^{db}* mouse model with PDE9a inhibition. qRT PCR was used to quantify expression of fibrosis associated genes (*Col1a2, Col3a1, Tgfb1, Mmp2, Loxl1, Loxl2 and Sparc*) as well as fetal gene markers (*Nppa, Nppb and MyH7*) in LV myocardium of *Lepr^{db}* mouse model with *Polr2a* as the reference gene. There are no significant differences of fibrotic genes between any of the experimental groups. There is an upregulation of *Myh7* in both groups of *Lepr$^{db/db}$* mice; however, there is no difference between *Lepr$^{db/db}$*-veh and *Lepr$^{db/db}$*-inh8. The result suggests no effect of PDE9a inhibition on fibrosis associated genes or fetal gene markers in *Lepr^{db}* model. * p≤0.05 n = 6,6,6,6 mice. Data were analyzed by two-way ANOVA without repeated measures followed by a Tukey test.

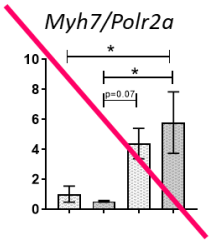

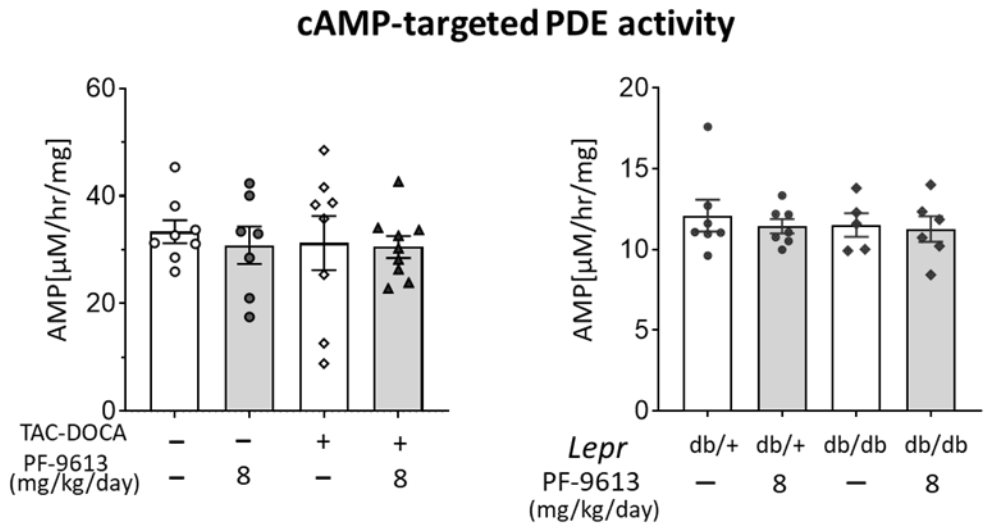

Supplemental Figure S5. cAMP-targeted PDE activity in LV myocardium. High performance liquid chromatography was used to assess cAMP-targeted PDEs in LV myocardial lysates. There is no alteration in cAMP-targeted PDE activity in any groups of mice that were treated with PDE9a inhibitor 8 mg/kg/day (n=8,7,8,9 mice for TAC-DOCA model, n= 7,7,5,6 for *Lepr*^{db} mice). Data were analyzed by two-way ANOVA without repeated measures followed by a Tukey test.

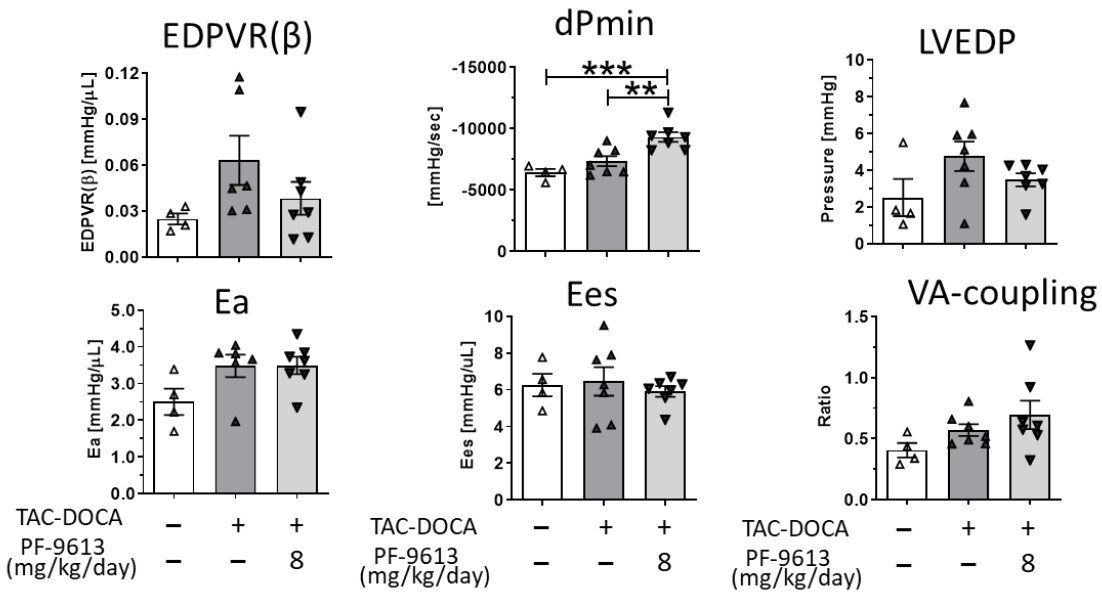

Supplemental Figure S6. Pressure volume analysis in a study of *female* TAC-DOCA mice. Female C57BL/6J mice at 4-5 months of ages were subjected to TAC-DOCA or sham surgery. At 1 week after surgery, mice had been subcutaneously implanted with osmotic minipumps containing either PDE9a inhibitor at 8 mg/kg/day or vehicle. At 5 weeks after surgery or 4 weeks after beginning of PDE9a inhibition, the animals were used for pressure-volume analysis. The results show a trend of diastolic improvement, reflected in parameters of PV analysis (trends of reduction in chamber stiffness (coefficient (β) of EDPVR) and lower LVEDP, and a significant increase in LV relaxation velocity (dPmin)) in the TAC-DOCA mice with PDE9a inhibition suggesting a possible beneficial effect of PDE9a inhibition on diastolic function; however, a trend of increased VA-coupling ratio also present suggesting possible VA discoordination. * p≤0.05 significant. n= 4,7,7 mice. Data were analyzed by one-way ANOVA without repeated measures followed by a Tukey test or Kruskal-Wallis followed by a Dunn test.

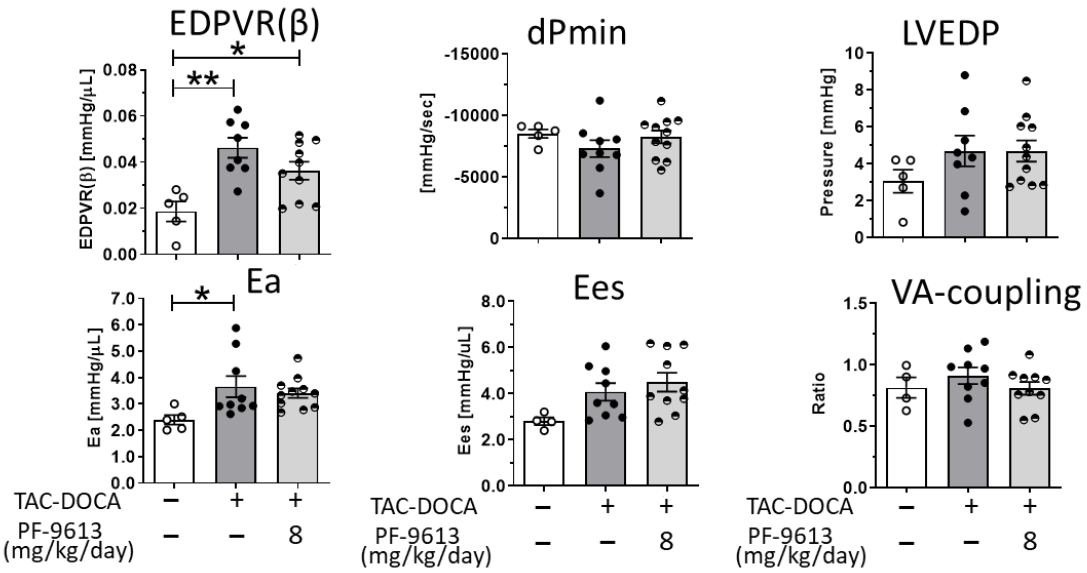

Supplemental Figure S7. Pressure volume analysis in *male* TAC-DOCA mice with <u>early initiation</u> of PDE9a inhibition. PDE9a inhibition has been initiated 1 week <u>prior</u> to the TAC-DOCA surgery and has been continued for 5 weeks after surgery (6 week total duration of PDE9a inhibition) in male C57BL/6J mice. At the end of week 6, pressure-volume analysis was performed to assess hemodynamic parameters. (Please note that in the main manuscript, the mice underwent TAC-DOCA surgery, then the PDE9a inhibitor was initiated 1 week <u>after surgery</u> and continued for 4 weeks). Mice treated with PDE9a inhibitor showed a trend of diastolic improvement, reflected in parameters of PV analysis (trends of reduction in chamber stiffness (coefficient (β) of EDPVR) and increase in LV relaxation velocity (dPmin)) compared to those treated with vehicle. Interestingly, initiation of PDE9a inhibition prior to surgery helped preserve LV contractility (Ees) and ventricular-arterial interaction (VA coupling ratio). * p≤0.05** p≤0.01 significant, n= 5,8,10 mice. Data were analyzed by one-way ANOVA without repeated measures followed by a Tukey test or Kruskal-Wallis followed by a Dunn test.

Supplemental References

1. Hu P, Zhang D, Swenson L, Chakrabarti G, Abel ED and Litwin SE. Minimally invasive aortic banding in mice: effects of altered cardiomyocyte insulin signaling during pressure overload. *Am J Physiol Heart Circ Physiol*. 2003;285:H1261-9.
2. Burkhoff D, Mirsky I and Suga H. Assessment of systolic and diastolic ventricular properties via pressure-volume analysis: a guide for clinical, translational, and basic researchers. *Am J Physiol Heart Circ Physiol*. 2005;289:H501-12.
3. Irving TC, Konhilas J, Perry D, Fischetti R and de Tombe PP. Myofilament lattice spacing as a function of sarcomere length in isolated rat myocardium. *American journal of physiology Heart and circulatory physiology*. 2000;279:H2568-73.
4. O'Connell TD, Rodrigo MC and Simpson PC. Isolation and culture of adult mouse cardiac myocytes. *Methods Mol Biol*. 2007;357:271-96.
5. Helmes M, Najafi A, Palmer BM, Breel E, Rijnveld N, Iannuzzi D and van der Velden J. Mimicking the cardiac cycle in intact cardiomyocytes using diastolic and systolic force clamps; measuring power output. *Cardiovascular research*. 2016;111:66-73.
6. Granzier HL and Irving TC. Passive tension in cardiac muscle: contribution of collagen, titin, microtubules, and intermediate filaments. *Biophysical journal*. 1995;68:1027-44.
7. Lee DI, Zhu G, Sasaki T, Cho GS, Hamdani N, Holewinski R, Jo SH, Danner T, Zhang M, Rainer PP, Bedja D, Kirk JA, Ranek MJ, Dostmann WR, Kwon C, Margulies KB, Van Eyk JE, Paulus WJ, Takimoto E and Kass DA. Phosphodiesterase 9A controls nitric-oxide-independent cGMP and hypertrophic heart disease. *Nature*. 2015;519:472-6.
8. Shah AM, Spurgeon HA, Sollott SJ, Talo A and Lakatta EG. 8-bromo-cGMP reduces the myofilament response to Ca2+ in intact cardiac myocytes. *Circulation research*. 1994;74:970-8.
9. Fisher DA, Smith JF, Pillar JS, St Denis SH and Cheng JB. Isolation and characterization of PDE9A, a novel human cGMP-specific phosphodiesterase. *J Biol Chem*. 1998;273:15559-64.
10. Oboh G, Adebayo AA, Ademosun AO and Boligon AA. In vitro inhibition of phosphodiesterase-5 and arginase activities from rat penile tissue by two Nigerian herbs (Hunteria umbellata and Anogeissus leiocarpus). *J Basic Clin Physiol Pharmacol*. 2017;28:393-401.
11. Oboh G, Ademiluyi AO, Oyeleye SI, Olasehinde TA and Boligon AA. Modulation of some markers of erectile dysfunction and malonaldehyde levels in isolated rat penile tissue with unripe and ripe plantain peels: identification of the constituents of the plants using HPLC. *Pharm Biol*. 2017;55:1920-1926.
12. Fawcett L, Baxendale R, Stacey P, McGrouther C, Harrow I, Soderling S, Hetman J, Beavo JA and Phillips SC. Molecular cloning and characterization of a distinct human phosphodiesterase gene family: PDE11A. *Proceedings of the National Academy of Sciences of the United States of America*. 2000;97:3702-7.
13. Bender AT and Beavo JA. Cyclic nucleotide phosphodiesterases: molecular regulation to clinical use. *Pharmacol Rev*. 2006;58:488-520.